Relativistic Prolapse-Free Gaussian Basis Sets of Quadruple-zeta Quality: (aug-)RPF-4Z. III. The f-Block Elements

Teodoro, Tiago Quevedo; Visscher, Lucas; Ferreira da Silva, Alberico Borges; Andrade Haiduke, Roberto Luiz

published in
Journal of Chemical Theory and Computation
2017

DOI (link to publisher)
10.1021/acs.jctc.6b00650

document version
Publisher's PDF, also known as Version of record

JCTC Journal of Chemical Theory and Computation

Article

pubs.acs.org/JCTC

Relativistic Prolapse-Free Gaussian Basis Sets of Quadruple-ζ Quality: (aug-)RPF-4Z. III. The f-Block Elements

Tiago Quevedo Teodoro,[†,‡] Lucas Visscher,[‡] Albérico Borges Ferreira da Silva,[†] and Roberto Luiz Andrade Haiduke*[,†]

[†]Department of Chemistry and Molecular Physics, São Carlos Institute of Chemistry, University of São Paulo, Trabalhador São-carlense Av. 400, São Carlos, Brazil

[‡]Amsterdam Center for Multiscale Modeling, Vrije Universiteit Amsterdam, de Boelelaan 1083, 1081 HV Amsterdam, The Netherlands

Supporting Information

ABSTRACT: The f-block elements are addressed in this third part of a series of prolapse-free basis sets of quadruple-ζ quality (RPF-4Z). Relativistic adapted Gaussian basis sets (RAGBSs) are used as primitive sets of functions while correlating/polarization (C/P) functions are chosen by analyzing energy lowerings upon basis set increments in Dirac−Coulomb multireference configuration interaction calculations with single and double excitations of the valence spinors. These function exponents are obtained by applying the RAGBS parameters in a polynomial expression. Moreover, through the choice of C/P characteristic exponents from functions of lower angular momentum spaces, a reduction in the computational demand is attained in relativistic calculations based on the kinetic balance condition. The present study thus complements the RPF-4Z sets for the whole periodic table (Z ≤ 118). The sets are available as Supporting Information and can also be found at http://basis-sets.iqsc.usp.br.

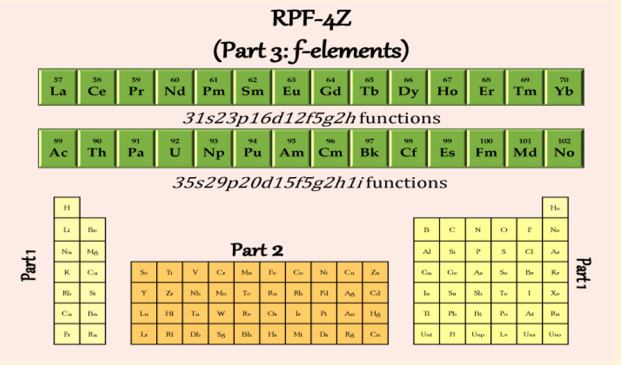

1. INTRODUCTION

The development of relativistic basis sets is complicated by the variational prolapse problem,[1] which arises from the fact that the Dirac−Hartree−Fock (DHF) energy is formally a saddle point rather than a minimum in the energy landscape. In the most severe cases, typically for heavy elements, this problem is readily identified by means of atomic DHF calculations resulting in energy values below accurate numerical data.[2] A more general test for prolapse relies on the identification of DHF energy increments upon addition of tight functions into a given set.[3] Signs of prolapse have been found in $s_{1/2}$ spinors of relativistic sets for elements as light as $_{37}$Rb.[4] Also, $p_{1/2}$ spinors are affected in some atoms of the sixth and seventh periods.[5,6] It is suggested that prolapse signs are related to an improper description of core-like electrons.[7] As the prolapse magnitude rapidly increases with nuclear charge increments, even valence-related properties of compounds containing superheavy elements should be investigated with care. As noticed by de Macedo et al.,[8] dissociation energies of darmstadtium carbide (DsC) from correlated calculations with prolapse-free and nonprolapse-free sets diverge by the order of the respective prolapse on the $_{110}$Ds basis set, approximately 17 kcal/mol. Thus, a consistent series of prolapse-free basis sets is useful for studying a broad range of properties and systems. One example of such a case is the relativistic adapted Gaussian basis set (RAGBS) series, which has been generated for the whole periodic table (Z ≤ 118).[4−6] Summarizing, the RAGBS function exponents (γ) of a given angular momentum l are determined through a polynomial equation[9]

$$\frac{\ln \gamma_i^{(l)}}{\alpha} = \Theta_{\min}^{(l)} + \sum_{q=1}^{3} \Delta\Theta_q^{(l)}(i-1)^q \quad (1)$$

where i = 1, 2, ..., N, with N being the number of discretization points (the number of functions in the set); α is a scaling parameter (used as 6.0); $\Theta_{\min}^{l}$ and $\Delta\Theta_{q=1,2,3}^{l}$ are the four polynomial parameters that define the mesh of discretization points. The polynomial parameters were obtained by minimizing the DHF energy. After this optimization, sets with signs of prolapse had the $\Delta\Theta_1^l$ parameter slightly increased in order to enlarge the spacing between adjacent exponent values. With this artifice, the exponents were displaced toward the innermost atomic regions until the DHF energy decreases along with further increments with tighter functions, which then eliminates the variational prolapse. The use of a polynomial for generating the RAGBSs also assures a well-behaved distribution of discretization points (exponents) as these sets yield DHF energies only a few milihartree (mHa) above accurate numerical results, even for the heaviest atoms.[6]

Received: June 28, 2016
Published: December 22, 2016

DOI: 10.1021/acs.jctc.6b00650
J. Chem. Theory Comput. 2017, 13, 1094−1101

In a recent series of papers, RAGBSs for elements of the *s*, *p*, and *d* blocks have been incremented with correlating/polarization (C/P) functions, giving rise to relativistic prolapse-free basis sets of quadruple-ζ quality (RPF-4Z).[10,11] The exponents of C/P functions in higher angular momentum spaces (l) than the ones already included in the RAGBSs are determined from the polynomial parameters that define the $l-2$ functions along with selected i integer values in eq 1. The methodology of repeating exponents in different angular momentum spaces is adopted for generating dual-family basis sets.[1] The number of small component functions generated by such sets is significantly reduced when applying the kinetic balance criterion[12,13] in relativistic calculations. One must notice though that the RPF series only uses this feature to obtain C/P functions, as all functions of angular momentum spaces in the primitive sets have been previously fully optimized.

Additionaly, atomic and molecular tests have also shown an excellent performance of the RPF-4Z series in comparison with successful quadruple-ζ sets available in the literature,[10,11] such as the ones developed by Dyall and co-workers (see ref 14 and references therein). This indicates that the RPF-4Z sets can likewise be used for general applications.

Here, we proceed to the RPF-4Z sets for the f-block elements in order to complement this series for the whole periodic table.

2. COMPUTATIONAL DETAILS

All calculations of the basis set incremental study were carried out with the four-component Dirac−Coulomb (DC) Hamiltonian as implemented within the DIRAC14 code[15] with the default Gaussian nuclear model[16] and speed of light value of 137.0359998 atomic units (au).[17] Two-electron integrals of small component functions, (SS|SS), have been replaced by an approximated interatomic energy correction in order to reduce the computational demand.[18] The kinetic balance condition is used for generating small component functions.[12,13] Multireference configuration interaction calculations (MRCI) were carried out with the direct relativistic configuration interaction module (DIRRCI).[19] The active space was set considering the ground-state electronic configuration of each atom.[20] Deep-core and subvalence spinors were frozen while $(n-2)f$, $(n-1)d$ (in atoms with at least one electron in these spinors), and ns spinors, with n being the main quantum number of the valence shell in each period, are included in the restricted active space 2 (RAS2). Remaining spinors with energy up to 100 au comprise RAS3. Single and double excitations from RAS2 to RAS3 were then considered (MRCISD) along with all possible excitations within RAS2. Thus, $Z-54$ and $Z-86$ electrons were correlated for the respective lanthanides and actinides.

Molecular calculations for a few diatomic molecules (LaF, LaCl, LaBr, LaI, CeO, CeS, PrN, AcF, AcCl, AcBr, AcI, ThO, ThS, and PaN) were also carried out with the DIRAC implementation of the spin-free exact-two-component (SF-X2C) Hamiltonian[21] at the coupled cluster level with single, double, and perturbative triple excitations (CCSD-T). The active space selected in these calculations included 18 valence electrons in each system and virtual spinors with energies up to 10 au. Seven points separated by 0.01 Å around the minimum of the potential energy curve for each molecule are used in a fourth-order polynomial fit through the TWOFIT utility program within the DIRAC package to obtain the equilibrium bond length (r_e) and harmonic vibrational frequency (ω_e) values. The electric dipole moment (μ_e) was obtained at the calculated r_e by adding the analytic value from DHF calculations and the contribution from electron correlation effects estimated through a finite-difference technique in a two-point form. The scalar factor attached to the dipole interaction term that was included into the Hamiltonian was set as 10^{-6} au.

The coupled cluster method with single and double substitutions has also been used here in Dirac−Coulomb Fock-space calculations (DC-FSCCSD) of excitation energies (using the (1,1) sector of Fock space) for the $_{70}$Yb and $_{102}$No atoms. The active space was set to include 24 valence electrons and virtual spinors with energy up to 10 au. The excitations were calculated on the basis of substitutions of the ns electrons to the $(n-1)d$ virtual spinors. We also take note that all calculations considered in this paper used basis sets in an uncontracted form.

3. RESULTS AND DISCUSSION

3.1. Basis Set Development. First, to illustrate how we choose the number of C/P functions and their exponents, compiled results for the basis set incremental study of the two closed-shell atoms in this series, $_{70}$Yb and $_{102}$No, are shown in Tables 1 and 2, respectively. Angular momentum spaces that are not included in the primitive RAGBSs (g, h, and i) are initially considered in order to compose a final set that *approaches* a quadruple-ζ type of incrementation. Thus, by first analyzing the data in Table 1, one can see that a usual quadruple-ζ incrementation with $3g2h1i$ functions does not yield a proper energy balance among such angular spaces. In the case of $_{70}$Yb, the "best" i function (i_4) yields an energy lowering of 5.94 mHa, which is still smaller than the effect of adding a fifth g function, 6.23 mHa, and only slightly above the result from adding a third h, 5.63 mHa. We observed that this outcome becomes even more pronounced for lighter elements, with the relative contribution from i functions decreasing toward the beginning of the series. Hence, by also considering the high computational demand associated with i functions, we decided not to include them in the final sets for lanthanides. Instead, sets with $5g$ and $2h$ functions seem to be a more adequate option for these elements in terms of energy balance. Such a different choice from the standard grouping of $3g2h1i$ functions is not surprising considering the size of correlating sets used in previous basis set developments in one- and two-component studies for lanthanides found in refs 22 and 23 and the dyall.vxz sets[24] in four-component calculations. However, the total size of these sets accounts for extra functions added in calculations in which the reference determinants from near-degenerate states are also considered. For example, dyall.v4z sets for the lanthanides include groupings of $3g2h1i$ functions on the basis of correlation of the $4f$ shell and $3f2g1h$ for correlation of the $5d6s$ shells. Even some other groupings are also added to account for the $4d$ correlation and $4f$ polarization. The latter methodology is completely justifiable when considering, for example, the near degeneracy of the [Xe]-$4f^{Z-56}6s^2$ and [Xe]$4f^{Z-57}5d^16s^2$ states of several atoms in the lanthanide series. When exponents of said $5d6s$ correlating functions are determined, low-lying states should be more properly treated, and the extra radial flexibility of these sets can further improve molecular data. On the other hand, in the present study, all correlating functions are determined only from calculations in which the reference determinants are constructed on the basis of the ground-state electronic configuration of each system. This means that reference

DOI: 10.1021/acs.jctc.6b00650
J. Chem. Theory Comput. 2017, 13, 1094−1101

Table 1. Incremental Study with Correlating Functions for the RAGBS of Ytterbium by Means of Energy Lowerings in DC-MRCISD Calculations[a]

set	exponent	E (Ha)	ΔE (mHa)
RAGBS[b]		−14069.22682	
$+1s_0$	9.9409×10^{-3}	−14069.22682	0.00
$+2s_{-1,0}$	3.0712×10^{-3}	−14069.22682	0.00
$+1p_0$	6.8873×10^{-2}	−14069.23457	−7.75
$+2p_{-1,0}$	2.3394×10^{-2}	−14069.23463	−7.81
$+3p_{-2,-1,0}$	7.1502×10^{-3}	−14069.23464	−7.82
$+1d_0$	3.6135×10^{-1}	−14069.23368	−6.86
$+2d_{-1,0}$	1.3527×10^{-1}	−14069.23573	−8.91
$+3d_{-2,-1,0}$	4.4500×10^{-2}	−14069.23596	−9.13
$+4d_{-3,...,0}$	1.2603×10^{-2}	−14069.23596	−9.14
$+1f_0$	6.2820×10^{-2}	−14069.22707	−0.25
$+2f_{-1,0}$	2.1106×10^{-2}	−14069.22708	−0.25
$+1g_0$	3.6135×10^{-1}	−14069.23320	−6.38
$+1g_1$	8.6601×10^{-1}	−14069.25399	−27.17
$+1g_2$	1.9008×10^{0}	−14069.30618	−79.36
$+1g_3$	3.9005×10^{0}	−14069.36807	−141.25
$+1g_4$	7.6390×10^{0}	−14069.37066	−143.84
$+1g_5$	1.4575×10^{1}	−14069.30598	−79.15
$+1g_6$	2.7660×10^{1}	−14069.24887	−22.05
$+2g_{3,4}$		−14069.43273	−205.91
$+3g_{2,3,4}$		−14069.46666	−239.84
$+4g_{2,...,5}$		−14069.49386	−267.04
$+5g_{1,...,5}$		−14069.50009	−273.26
$+6g_{1,...,6}$		−14069.50266	−275.83
$+1h_1$	1.6854×10^{-1}	−14069.22695	−0.13
$+1h_2$	4.1468×10^{-1}	−14069.22712	−0.30
$+1h_3$	9.5180×10^{-1}	−14069.22910	−2.28
$+1h_4$	2.0732×10^{0}	−14069.23743	−10.61
$+1h_5$	4.3600×10^{0}	−14069.25079	−23.97
$+1h_6$	9.0055×10^{0}	−14069.25352	−26.70
$+1h_7$	1.8584×10^{1}	−14069.24164	−14.82
$+2h_{5,6}$		−14069.26737	−40.55
$+3h_{5,6,7}$		−14069.27300	−46.18
$+1i_1$	8.6601×10^{-1}	−14069.22695	−0.13
$+1i_2$	1.9008×10^{0}	−14069.22898	−2.16
$+1i_3$	3.9005×10^{0}	−14069.23182	−5.00
$+1i_4$	7.6390×10^{0}	−14069.23276	−5.94
$+1i_5$	1.4575×10^{1}	−14069.23101	−4.19

[a]Indexes in the first column refer to i value(s) to be used in eq 1 along with the respective RAGBS parameters[5] (l parameters for angular momentum spaces already included in the RAGBSs and $l-2$ parameters for higher angular momentum functions). [b]Basis set size of 30s21p13d11f functions.

Table 2. Incremental Study with Correlating Functions for the RAGBS of Nobelium by Means of Energy Lowerings in DC-MRCISD Calculations[a]

set	exponent	E (Ha)	ΔE (mHa)
RAGBS[b]		−36753.21762	
$+1s_0$	1.1133×10^{-2}	−36753.21762	0.00
$+2s_{-1,0}$	3.2412×10^{-3}	−36753.21762	0.00
$+1p_0$	6.0866×10^{-2}	−36753.22412	−6.50
$+2p_{-1,0}$	2.0089×10^{-2}	−36753.22413	−6.51
$+1d_0$	3.5390×10^{-1}	−36753.23227	−14.65
$+2d_{-1,0}$	1.3020×10^{-1}	−36753.23580	−18.18
$+3d_{-2,-1,0}$	4.2030×10^{-2}	−36753.23615	−18.53
$+4d_{-3,...,0}$	1.1713×10^{-2}	−36753.23616	−18.54
$+1f_0$	6.0915×10^{-2}	−36753.21782	−0.20
$+2f_{-1,0}$	2.0243×10^{-2}	−36753.21782	−0.20
$+1g_{-1}$	1.3020×10^{-1}	−36753.21954	−1.92
$+1g_0$	3.5390×10^{-1}	−36753.23531	−17.69
$+1g_1$	8.5798×10^{-1}	−36753.30399	−86.37
$+1g_2$	1.8858×10^{0}	−36753.43015	−212.53
$+1g_3$	3.8195×10^{0}	−36753.42962	−212.00
$+1g_4$	7.2463×10^{0}	−36753.28150	−63.88
$+1g_5$	1.3089×10^{0}	−36753.22116	−3.55
$+2g_{2,3}$		−36753.51961	−301.99
$+3g_{1,2,3}$		−36753.54674	−329.12
$+4g_{1,...,4}$		−36753.56376	−346.14
$+5g_{0,...,4}$		−36753.56619	−348.57
$+1h_2$	4.0084×10^{-1}	−36753.21846	−0.84
$+1h_3$	9.0334×10^{-1}	−36753.22456	−6.94
$+1h_4$	1.9052×10^{0}	−36753.24567	−28.05
$+1h_5$	3.8177×10^{0}	−36753.25843	−40.81
$+1h_6$	7.3785×10^{0}	−36753.23589	−18.27
$+1h_7$	1.3962×10^{0}	−36753.21956	−1.94
$+2h_{4,5}$		−36753.26970	−52.08
$+3h_{4,5,6}$		−36753.27389	−56.27
$+1i_1$	8.5798×10^{-1}	−36753.21971	−2.09
$+1i_2$	1.8858×10^{0}	−36753.22457	−6.96
$+1i_3$	3.8195×10^{0}	−36753.22762	−10.00
$+1i_4$	7.2463×10^{0}	−36753.22278	−5.16
$+2i_{2,3}$		−36753.23100	−13.38

[a]Indexes in the first column refer to i value(s) to be used in eq 1 along with the respective RAGBS parameters[6] (l parameters for angular momentum spaces already included in the RAGBSs and $l-2$ parameters for higher angular momentum functions). [b]Basis set size of 33s27p17d14f functions.

determinants for lanthanides heavier than Z = 58 (with exception of Gd) do not account for the [Xe]$4f^{Z-57}5d^16s^2$ configuration. This was done as, first, we mean to keep consistency with the methodology applied to construct the RPF-4Z sets for elements in other groups. Also, as we determine exponents by means of the polynomial in eq 1 along with predetermined parameters, the choices of exponent values are rather limited, which reduces the effect of changing parameters such as including other reference states. Finally, adding extra functions to avoid this possible bias toward a specific configuration, which in the present study is the ground-state configuration, could make these sets computationally too demanding and with little gain in the description of general properties (this will be further discussed in section 3.2).

Regarding the choice of exponents, the indexes associated with the optimum 5g and 2h functions for $_{70}$Yb are i = 1, ...,5 and i = 5, 6, respectively, The same trend is kept throughout almost the whole series of lanthanides with a regular [Xe]$4f^{Z-56}6s^2$ electronic configuration. The only exception is $_{59}$Pr, which showed a different pattern of indexes for g functions, yielding more diffuse exponents (i = 0, ...,4). This is expected as one considers the atomic radii contraction along the lanthanide series. Moreover, even though the indexes for the h functions do not change, their respective exponents for the $_{70}$Yb set (chosen from the f subset) are overall tighter than the corresponding ones for the $_{59}$Pr set (the most diffuse exponent in each case is 0.16854 and 0.079817, respectively). The elements with an irregular ground-state electronic configuration, $_{57}$La ([Xe]$5d^16s^2$) and $_{58}$Ce ([Xe]$4f^15d^16s^2$), showed optimum indexes distinct from those found for the other lanthanides, although a tendency to more diffuse

DOI: 10.1021/acs.jctc.6b00650
J. Chem. Theory Comput. 2017, 13, 1094−1101

Table 3. Selected Indexes for the Correlating/Polarization Functions of the Lanthanide Sets[a]

element	elec. config.	*s*	*p*	*d*	*f*	*g*	*h*
$_{57}$La	[Xe]$5d^16s^2$	0	−1, 0	0	0, ..., 11	1, ..., 5	1, 2
$_{58}$Ce	[Xe]$4f^15d^16s^2$	0	−1, 0	0	0	1, ..., 5	2, 3
$_{59}$Pr	[Xe]$4f^36s^2$	0	−1, 0	−2, −1, 0	0	0, ..., 4	5, 6
$_{60}$Nd	[Xe]$4f^46s^2$	0	−1, 0	−2, −1, 0	0	1, ..., 5	5, 6
$_{61}$Pm	[Xe]$4f^56s^2$	0	−1, 0	−2, −1, 0	0	1, ..., 5	5, 6
$_{62}$Sm	[Xe]$4f^66s^2$	0	−1, 0	−2, −1, 0	0	1, ..., 5	5, 6
$_{63}$Eu	[Xe]$4f^76s^2$	0	−1, 0	−2, −1, 0	0	1, ..., 5	5, 6
$_{64}$Gd	[Xe]$4f^75d^16s^2$	0	−1, 0	0	0	2, ..., 6	3, 4
$_{65}$Tb	[Xe]$4f^96s^2$	0	−1, 0	−2, −1, 0	0	1, ..., 5	5, 6
$_{66}$Dy	[Xe]$4f^{10}6s^2$	0	−1, 0	−2, −1, 0	0	1, ..., 5	5, 6
$_{67}$Ho	[Xe]$4f^{11}6s^2$	0	−1, 0	−2, −1, 0	0	1, ..., 5	5, 6
$_{68}$Er	[Xe]$4f^{12}6s^2$	0	−1, 0	−2, −1, 0	0	1, ..., 5	5, 6
$_{69}$Tm	[Xe]$4f^{13}6s^2$	0	−1, 0	−2, −1, 0	0	1, ..., 5	5, 6
$_{70}$Yb	[Xe]$4f^{14}6s^2$	0	−1, 0	−2, −1, 0	0	1, ..., 5	5, 6

[a]The indexes correspond to the *i* values to be used in eq 1 along with the respective RAGBS parameters[5] (*l* parameters for angular momentum spaces already included in the RAGBSs and *l*−2 parameters for higher angular momentum functions).

Table 4. Selected Indexes for the Correlating/Polarization Functions of the Actinide Sets[a]

element	elec. config.	*s*	*p*	*d*	*f*	*g*	*h*	*i*
$_{89}$Ac	[Rn]$6d^17s^2$	−1, 0	−1, 0	0	−2, −1, 0, 12	1, ..., 5	0, 1	2
$_{90}$Th	[Rn]$6d^27s^2$	−1, 0	−1, 0	0	−2, −1, 0, 12	1, ..., 5	0, 1	3
$_{91}$Pa	[Rn]$5f^26d^17s^2$	−1, 0	−1, 0	0	0	2, ..., 6	3, 4	4
$_{92}$U	[Rn]$5f^36d^17s^2$	−1, 0	−1, 0	0	0	2, ..., 6	4, 5	4
$_{93}$Np	[Rn]$5f^46d^17s^2$	−1, 0	−1, 0	0	0	2, ..., 6	4, 5	5
$_{94}$Pu	[Rn]$5f^67s^2$	−1, 0	−1, 0	−2, −1, 0	0	−1, ..., 3	4, 5	2
$_{95}$Am	[Rn]$5f^77s^2$	−1, 0	−1, 0	−2, −1, 0	0	0, ..., 4	4, 5	2
$_{96}$Cm	[Rn]$5f^76d^17s^2$	−1, 0	−1, 0	0	0	2, ..., 6	4, 5	5
$_{97}$Bk	[Rn]$5f^97s^2$	−1, 0	−1, 0	−2, −1, 0	0	0, ..., 4	4, 5	2
$_{98}$Cf	[Rn]$5f^{10}7s^2$	−1, 0	−1, 0	−2, −1, 0	0	0, ..., 4	4, 5	3
$_{99}$Es	[Rn]$5f^{11}7s^2$	−1, 0	−1, 0	−2, −1, 0	0	0, ..., 4	4, 5	3
$_{100}$Fm	[Rn]$5f^{12}7s^2$	−1, 0	−1, 0	−2, −1, 0	0	0, ..., 4	4, 5	3
$_{101}$Md	[Rn]$5f^{13}7s^2$	−1, 0	−1, 0	−2, −1, 0	0	0, ..., 4	4, 5	3
$_{102}$No	[Rn]$5f^{14}7s^2$	−1, 0	−1, 0	−2, −1, 0	0	0, ..., 4	4, 5	3

[a]The indexes correspond to the *i* values to be used in eq 1 along with the respective RAGBS parameters[6] (*l* parameters for angular momentum spaces already included in the RAGBSs and *l*−2 parameters for higher angular momentum functions).

functions with decreasing atomic number is still observed. Results for $_{64}$Gd ([Xe]$4f^75d^16s^2$) were extrapolated on the basis of those for $_{58}$Ce.

Although the exponents analyzed here are limited by the integer *i* values applied in eq 1, the optimum values chosen are still in overall agreement with the ones from fully optimized basis sets, such as those from the dyall.v4z sets. For example, the 3*g*, 2*h*, and 1*i* dyall.v4z function exponents for $_{70}$Yb (from 4*f* excitations) are 1.93167, 5.84306, and 16.9300; 3.89459 and 12.0159; and 7.82630, respectively. These values are similar to exponents selected in Table 1. On the other hand, by using a 5*g*2*h* set with the same exponents as functions already found in lower angular momentum spaces, a reduction of 80 small component Cartesian basis functions is attained with the kinetic balance condition in comparison with a fully optimized set of the same size. This represents approximately 10% of the total number of these functions in calculations with sets around the size of the ones considered here, a reduction that will obviously provide better computational efficiency for the RPF-4Z sets.

Another aspect to take into account during the development of the RPF-4Z sets concerns the eventual need for additional functions in angular momentum spaces already considered in the RAGBSs. More diffuse functions in such symmetries may be required for correlated treatments, and its relevance can not be adequately accessed in Hartree−Fock calculations, which were used to generate the primitive sets. On the basis of results in the first papers of the series and on the effect of such diffuse functions to molecular properties, we adopted a threshold of 10^{-2} mHa in the energy lowerings in order to include any of these extra functions. Results in Table 1 suggest that 2*p*, 3*d*, and 1*f* diffuse functions would be necessary for $_{70}$Yb. Again, the same pattern stands for other elements with the same regular electronic configuration. Furthermore, as the initial RAGBSs of $_{57}$La, $_{58}$Ce, and $_{64}$Gd already contain two more *d* functions than the sets of elements with regular electronic configurations, only one extra *d* function was necessary in these cases (energy variations above 10^{-2} mHa). This is consistent with a family of basis sets that is expected to have a constant size throughout a whole sub-block. Additionally, analyses of the sets for the lightest lanthanides also showed energy lowerings above the 10^{-2} mHa threshold for the first diffuse *s* function, which is related to the diffuseness of the *s* spinors in these elements. Hence, to increase the radial flexibility of these sets and to maintain their sizes constant through the sub-block, one extra *s*

DOI: 10.1021/acs.jctc.6b00650
J. Chem. Theory Comput. 2017, 13, 1094−1101

function was also added to the sets of other lanthanides. The final RPF-4Z sets for the lanthanides are therefore composed of 31*s*23*p*16*d*12*f*5*g*2*h* functions. Indexes associated with the C/P functions of all these sets are shown in Table 3.

The largest energy variation caused by an *i* function for $_{102}$No, 10.00 mHa (i_3) is now more significant as its effect is larger than that of a fifth *g* (2.43 mHa) and a third *h* (4.18 mHa) function (see Table 2). Once more, a similar trend was noticed for lighter elements. However, energy lowerings yielded by a fifth *g* function are sometimes as significant for other actinides as those for the optimum *i* function, which is the reason for selecting 5*g*2*h*1*i* functions of such angular momentum for these elements. Again, correlating sets with different sizes from the standard 3*g*2*h*1*i* are also used to compose other basis functions for actinides such as those in refs 25−27. As also shown in Table 2, the number of functions with low angular momentum follows a pattern similar to that observed for $_{70}$Yb in terms of energy lowerings above the threshold of 10^{-2} mHa, but with one less *p* function for heavier actinides. Hence, 1*p*3*d*1*f* functions would be recommended for the actinides. Nevertheless, results for elements in the beginning of the actinide series show that a second *p* and also two *s* diffuse functions also yield energy lowerings above the threshold. Then, for a better radial flexibility of these sets and to keep the same size along the whole sub-block, the RPF-4Z sets for all actinides comprise 35*s*29*p*20*d*15*f*5*g*2*h*1*i* functions. The indexes used to generate the C/P functions of these sets are displayed in Table 4.

3.2. Molecular and Atomic Tests. The RPF-4Z series has been evaluated in molecular calculations of standard spectroscopic and electric properties against experimental data and theoretical values obtained with other basis sets. Unfortunately, accurate experimental results for simple molecules containing f-block elements are scarce, and studies with larger molecules are beyond the scope of the present paper. Thus, we consider only a few diatomic molecules containing the first three elements of each lanthanide and actinide series and nonmetals of the main group. Results for r_e are displayed in Table 5 along with experimental data.[28,29]

Table 5. Equilibrium Bond Length (Å), r_e, of Diatomic Molecules at the Ground State Calculated at the X2C(SF)-CCSD-T Level of Theory with Different Basis Sets and Experimental Data[a]

	dyall.v3z	dyall.v4z	RPF-4Z	exptl.
LaF	2.071	2.061	2.031	2.023
LaCl	2.546	2.533	2.506	2.498
LaBr	2.703	2.688	2.667	2.652
LaI	2.936	2.918	2.900	2.879
CeO	1.750	1.744	1.746	
CeS	2.244	2.227	2.231	
PrN	1.749	1.740	1.741	
AcF	2.141	2.123	2.116	
AcCl	DNC[b]	2.628	2.618	
AcBr	2.813	2.793	2.788	
AcI	3.061	3.041	3.037	
ThO	1.849	1.847	1.850	1.840
ThS	2.357	2.354	2.357	
PaN	1.746	1.744	1.742	

[a]Experimental data taken from refs 28 and 29. [b]CC energy did not converge.

First, by observing the r_e values calculated with the Dyall sets, there is a common pattern of shortening bond lengths from dyall.v3z to dyall.v4z results. Convergence is also seen toward experimental data for the lanthanum halides and ThO. One can also notice a clear improvement of results given by the RPF-4Z set for lanthanum halides in comparison with those from the dyall.vxz sets. Results from the RPF-4Z set for these systems show equilibrium bond lengths on average 2.4 pm closer to experimental data than the ones from calculations with the dyall.v4z set. A similar trend is noticed for actinium halides, as r_e determinations when calculated with the RPF-4Z set are 0.7 pm shorter than with the dyall.v4z one. For the remaining lanthanide-containing molecules, results from the RPF-4Z set indicate bonds that are slightly longer than those found with the dyall.v4z calculations by an average of 0.2 pm but still considerably shorter than those obtained with the dyall.v3z set (by 0.8 pm). Results for ThO and ThS show a different pattern as slightly larger bond lengths are obtained with the RPF-4Z set with respect to those from both dyall.vxz sets, while the former pattern is seen again for PaN. However, differences between results with any of these analyzed sets are rather small for these molecules, 0.3 pm at most.

To better understand the latter results one must look for differences in the exponents of these sets or, in a more general manner, their size. In Table 6 we present the number of primitive Cartesian functions generated in calculations for molecules analyzed above. The total number of such functions in calculations with the RPF-4Z sets is always between what is obtained with the dyall.v3z and dyall.v4z sets, with a closer value to the latter in calculations for lanthanum- and actinium-containing molecules. This arises from the fact that whereas the RPF-4Z sets are presented with a constant size along each sub-block, the dyall.vxz sets contain fewer functions for lanthanum and actinium, as these atoms are treated as d-block elements. The advantage of the *dual-family* scheme for generating correlating functions in the RPF-4Z series must be noticed at this point. When exponents from the primitive set are repeated in the correlating groups, a smaller number of small-component functions is generated upon use of the kinetic balance condition in relativistic calculations. Such a feature is clear for lanthanum-containing molecules as the total number of primitive Cartesian

Table 6. Total Number of Cartesian Primitive Functions (of Which the Number of Large Component Ones Are Shown in Parentheses) Generated with Different Basis Sets for Molecules Analysed in the Present Study

	dyall.v3z	dyall.v4z	RPF-4Z
LaF	1008 (303)	1605 (492)	1516 (527)
LaCl	1054 (316)	1669 (510)	1572 (543)
LaBr	1276 (384)	1953 (597)	1785 (606)
LaI	1441 (434)	2120 (648)	1898 (640)
CeO	1476 (455)	2087 (649)	1588 (527)
CeS	1522 (468)	2151 (667)	1644 (543)
PrN	1476 (455)	2133 (664)	1588 (527)
AcF	1502 (460)	2120 (656)	1897 (631)
AcCl	1548 (473)	2184 (674)	1953 (647)
AcBr	1770 (541)	2468 (761)	2166 (710)
AcI	1935 (591)	2635 (812)	2279 (744)
ThO	1704 (526)	2512 (785)	1897 (631)
ThS	1750 (539)	2576 (803)	1953 (647)
PaN	1722 (532)	2512 (785)	1897 (631)

DOI: 10.1021/acs.jctc.6b00650
J. Chem. Theory Comput. 2017, 13, 1094−1101

functions associated with calculations applying the RPF-4Z set is smaller than the number of functions generated by the dyall.v4z set, even though the number of large-component functions is greater with the former. Overall, the analysis for r_e shows that the RPF-4Z sets are capable of providing results as precise as those obtained with the dyall.v4z sets, but with a smaller total number of functions.

Harmonic vibrational frequencies presented in Table 7 also show a convergent pattern when the basis set size increases within a series. Thus, ω_e values decrease as going from the dyall.v4z set to the dyall.v3z one (with ThO being the only exception). The main trend of increasing ω_e values with larger sets is in part explained by shorter bond lengths. Nevertheless, results from calculations with the RPF-4Z set are in almost all cases closer to data associated with the dyall.v4z set than with the dyall.v3z one.

Table 7. Harmonic Vibrational Frequencies (cm^{-1}), ω_e, of Diatomic Molecules at the Ground State Calculated at the X2C(SF)-CCSD-T Level of Theory with Different Basis Sets and Experimental Data[a]

	dyall.v3z	dyall.v4z	RPF-4Z	exptl.
LaF	561.6	562.9	566.0	574.9
LaCl	337.6	340.3	347.3	341.4
LaBr	232.2	235.3	237.9	236.2
LaI	181.3	184.5	185.8	189.5
CeO	924.0	937.4	936.0	
CeS	373.3	475.0	450.3	
PrN	861.1	869.9	860.9	
AcF	527.2	532.9	539.2	
AcCl	DNC[b]	309.1	314.5	
AcBr	202.2	204.9	206.3	
AcI	152.9	155.0	155.6	
ThO	892.8	889.9	888.6	895.8
ThS	482.6	484.6	485.5	
PaN	1102	1105	1107	

[a]Experimental data taken from refs 28 and 29. [b]CC energy did not converge.

Regarding the electric dipole moments in Table 8, there is not a clear pattern of such results with respect to basis set sizes, indicating that μ_e values are even more sensitive to minute changes of the sets than the spectroscopic properties considered before. The experimental values for LaF and ThO are between theoretical results calculated with the dyall.v4z and RPF-4Z sets.[30,31] For ThS, theoretical data are virtually the same with the two quadruple-ζ sets, both indicating a μ_e value approximately 0.1 D above the experimental result.[32] In all three cases, the largest deviation with respect to experimental data is observed with the dyall.v3z set. The lack of accurate experimental data for other f-block systems does not allow a further comparison with experiments. However, when these three systems along with others containing atoms of different blocks of the periodic table are considered,[10,11] there is strong evidence that the RPF-4Z sets are also capable of providing results at least as accurate as those obtained with the dyall.v4z sets for this fundamental electric property.

Another consideration that is made concerns the active space used here for determining the correlating groups of functions. As previously discussed, reference determinants account for only the ground-state electronic configuration of each system. This could imply a bias toward the f-configurations (as the static correlation energy in calculations for determining the ideal grouping of correlating functions for, e.g., Pr does not consider 5*d* spinors). Such possible deficiency does not appear to be severe from the spectroscopic and electric data among lanthanide-containing molecules. Even though correlating groups of functions for $_{57}$La, $_{58}$Ce, and $_{59}$Pr were determined on the basis of different ground-state configurations, [Xe]-$5d^16s^2$, [Xe]$4f^15d^16s^2$, and [Xe]$4f^36s^2$, respectively, all properties obtained with the RPF-4Z set show overall values in close agreement with those from calculations with the dyall.v4z set, which additionally includes groupings of correlating functions for different types of excitations. To further check for this possible bias we carried out Fock-space coupled cluster calculations of excitation energies for $_{70}$Yb and $_{70}$No from the *ns* to $(n-1)d$ spinors (with *n* being the main quantum number of the valence shell). As we considered excitations only from the $(n-2)f$ and *ns* shells to determine the correlating functions of the RPF-4Z sets, one could expect the treatment of an excited state in which electrons are included in the $(n-1)d$ shell should not be as accurate as what is obtained with the dyall.vxz sets. However, as one can notice from results displayed in Table 9, excitation energies for $_{70}$Yb are consistent among calculations with the different sets and experimental data. Results obtained with the RPF-4Z set stand between data from the dyall.vxz sets, only about 4−5% higher than values from calculations with the dyall.v4z set for the ^{3}D terms. For $_{102}$No (Table 10), although excitation energies determined with the RPF-4Z set are larger than those from the dyall.vxz sets, the

Table 8. Electric Dipole Moments (D), u_e, of Diatomic Molecules at the Ground State Calculated at the SF-X2C−CCSD-T Level of Theory with Different Basis Sets and Experimental Data[a]

	dyall.v3z	dyall.v4z	RPF-4Z	exptl.
LaF	2.137	2.057	1.729	1.808
LaCl	3.469	3.568	3.278	
LaBr	3.707	3.847	3.687	
LaI	4.041	4.246	4.147	
CeO	0.554	0.526	0.575	
CeS	2.855	2.716	2.760	
PrN	6.643	6.595	6.631	
AcF	2.431	2.287	2.241	
AcCl	DNC[b]	3.571	3.469	
AcBr	3.831	3.807	3.797	
AcI	4.089	4.083	4.086	
ThO	2.745	2.763	2.814	2.782
ThS	4.498	4.593	4.591	4.58
PaN	3.110	3.153	3.072	

[a]Experimental data taken from refs. 30−32. [b]CC energy did not converge.

Table 9. Excitation Energies (cm^{-1}) of the $_{70}$Yb Atom Calculated at the DC-FSCCSD Level of Theory with Different Basis Sets and Experimental Data[a]

configuration	term	J	dyall.v3z	dyall.v4z	RPF-4Z	exptl.
$4f^{14}5d6s$	^{3}D	1	25373	23923	25044	24489
		2	25623	24249	25328	24752
		3	26238	24905	25946	25271
	^{1}D	2	28024	28015	28270	27678

[a]Experimental data taken from ref 29.

DOI: 10.1021/acs.jctc.6b00650
J. Chem. Theory Comput. 2017, 13, 1094−1101

Table 10. Excitation Energies (cm^{-1}) of the $_{102}$No Atom Calculated at the DC-FSCCSD Level of Theory with Different Basis Sets

configuration	term	J	dyall.v3z	dyall.v4z	RPF-4Z
$5f^{14}6d7s$	^{3}D	1	28020	27709	28328
		2	28640	28359	28937
		3	30134	29765	30437
	^{1}D	2	33967	34421	34114

differences to the dyall.v4z results are even smaller than those found for $_{70}$Yb, only about 2% higher for the ^{3}D terms.

Finally, regarding the choice of active space in atomic and molecular calculations, it is common to include subvalence $(n-1)sp$ spinors in the active space because these shells are quite polarizable. As shown above, we find in our calculations consistent results when correlating electrons in these shells, even though exponents were not explicitly optimized to describe this kind of core−valence correlation. This provides an economical alternative to the explicitly optimized exponents that are included in the dyall.vxz sets.

3.3. aug-RPF-4Z. Another advantage of the sets provided here is that one can easily obtain extra functions (exponents) for more specific studies by means of the polynomial expression in eq 1 with predetermined parameters.[4−6] In a recent paper we calculated electric field gradients at the potassium nuclei with a modified version of the RPF-4Z set for that element in which tighter functions were generated by using the polynomial parameters in a consistent manner.[33] Augmented versions of the RPF-4Z sets have also been provided in a ready-to-implement format by adding one extra diffuse function to every angular momentum space. This alternative version is recommended for studies of anions and/or systems with long-range interactions. The aug-RPF-4Z basis sets for the f-elements are also available as Supporting Information files and at http://basis-sets.iqsc.usp.br.

4. CONCLUSION

The RPF-4Z sets generated here for f-block elements were tested in two-component molecular and four-component atomic calculations. Results are overall consistent with data obtained by applying the standard relativistic dyall.v4z sets. Through repetition of exponents in the correlating sets from functions in lower angular momentum spaces, in addition to a distribution of points in the primitive set determined through a polynomial, the RPF-4Z sets generates a reduced and efficient number of total primitive Cartesian functions with respect to fully optimized sets. In addition to such efficiency, the implications of the prolapse issue can be further studied in a broad range of systems with this new form of polarized prolapse-free sets of quadruple-ζ quality provided for the whole periodic table.

■ ASSOCIATED CONTENT

Supporting Information

The Supporting Information is available free of charge on the ACS Publications website at DOI: 10.1021/acs.jctc.6b00650.

RPF-4Z sets for the f-block elements in a ready-to-implement format (TXT)

aug-RPF-4Z sets for the f-block elements in a ready-to-implement format (TXT)

■ AUTHOR INFORMATION

Corresponding Author

*E-mail: haiduke@iqsc.usp.br.

Funding

T.Q.T. thanks FAPESP (São Paulo Research Foundation) for a doctoral fellowship (Grant 2012/22143-5) and a research fund (Grant 2014/02939-5). T.Q.T. and R.L.A.H. also acknowledge FAPESP for financial support (Grant 2010/18743-1 and 2014/23714-1). This work was sponsored by NWO Physical Sciences for the use of supercomputer facilities.

Notes

The authors declare no competing financial interest.

■ REFERENCES

(1) Fægri, K., Jr. *Theor. Chem. Acc.* **2001**, *105*, 252−258.
(2) Dyall, K. G. *Chem. Phys.* **2012**, *395*, 35−43.
(3) Tatewaki, H.; Koga, T.; Mochizuki, Y. *Chem. Phys. Lett.* **2003**, *375*, 399−405.
(4) Haiduke, R. L. A.; da Silva, A. B. F. *J. Comput. Chem.* **2006**, *27*, 61−71.
(5) Haiduke, R. L. A.; da Silva, A. B. F. *J. Comput. Chem.* **2006**, *27*, 1970−1979.
(6) Teodoro, T. Q.; Haiduke, R. L. A. *J. Comput. Chem.* **2013**, *34*, 2372−2379.
(7) Tatewaki, H.; Mochizuki, Y. *Theor. Chem. Acc.* **2003**, *109*, 40−42.
(8) de Macedo, L. G. M.; Sambrano, J. R.; de Souza, A. R.; Borin, A. C. *Chem. Phys. Lett.* **2007**, *440*, 367−371.
(9) Haiduke, R. L. A.; de Macedo, L. G. M.; Barbosa, R. C.; da Silva, A. B. F. *J. Comput. Chem.* **2004**, *25*, 1904−1909.
(10) Teodoro, T. Q.; da Silva, A. B. F.; Haiduke, R. L. A. *J. Chem. Theory Comput.* **2014**, *10*, 3800−3806.
(11) Teodoro, T. Q.; da Silva, A. B. F.; Haiduke, R. L. A. *J. Chem. Theory Comput.* **2014**, *10*, 4761−4764.
(12) Stanton, R. E.; Havriliak, S. *J. Chem. Phys.* **1984**, *81*, 1910−1918.
(13) Lee, Y. S.; McLean, A. D. *J. Chem. Phys.* **1982**, *76*, 735−736.
(14) Dyall, K. G. *Theor. Chem. Acc.* **2012**, *131*, 1−20.
(15) DIRAC, a relativistic ab initio electronic structure program, Release DIRAC14 (2014), written by Saue, T.; Visscher, L.; Jensen, H. J. Aa.; Bast, R. with contributions from Bakken, V.; Dyall, K. G.; Dubillard, S.; Ekström, U.; Eliav, E.; Enevoldsen, T.; Faßhauer, E.; Fleig, T.; Fossgaard, O.; Gomes, A. S. P.; Helgaker, T.; Lærdahl, J. K.; Lee, Y. S.; Henriksson, J.; Iliaš, M.; Jacob, Ch. R.; Knecht, S.; Komorovský, S.; Kullie, O.; Larsen, C. V.; Nataraj, H. S.; Norman, P.; Olejniczak, G.; Olsen, J.; Park, Y. C.; Pedersen, J. K.; Pernpointner, M.; di Remigio, R.; Ruud, K.; Sałek, P.; Schimmelpfennig, B.; Sikkema, J.; Thorvaldsen, A. J.; Thyssen, J.; van Stralen, J.; Villaume, S.; Visser, O.; Winther, T.; Yamamoto, S. (see http://www.diracprogram.org, accessed on 05/30/2016).
(16) Visscher, L.; Dyall, K. G. *At. Data Nucl. Data Tables* **1997**, *67*, 207−224.
(17) Mohr, P. J.; Taylor, B. N. *J. Phys. Chem. Ref. Data* **1999**, *28*, 1713−1852.
(18) Visscher, L. *Theor. Chem. Acc.* **1997**, *98*, 68−70.
(19) Visscher, L.; Visser, O.; Aerts, P. J. C.; Merenga, H.; Nieuwpoort, W. C. *Comput. Phys. Commun.* **1994**, *81*, 120.
(20) Haynes, W. M. *CRC Handbook of Chemistry and Physics*; CRC Press: Boca Raton, FL, 2016; pp 9−160.
(21) Iliaš, M.; Saue, T. *J. Chem. Phys.* **2007**, *126*, 064102.
(22) Roos, B. O.; Lindh, R.; Malmqvist, P.-Å.; Veryazov, V.; Widmark, P.-O.; Borin, A. C. *J. Phys. Chem. A* **2008**, *112*, 11431−11435.
(23) Gulde, R.; Pollak, P.; Weigend, F. *J. Chem. Theory Comput.* **2012**, *8*, 4062−4068.
(24) Gomes, A. S.; Dyall, K. G.; Visscher, L. *Theor. Chem. Acc.* **2010**, *127*, 369−381.
(25) Peterson, K. A. *J. Chem. Phys.* **2015**, *142*, 074105.

DOI: 10.1021/acs.jctc.6b00650
J. Chem. Theory Comput. 2017, 13, 1094−1101

(26) Roos, B. O.; Lindh, R.; Malmqvist, P.-Å.; Veryazov, V.; Widmark, P.-O. *Chem. Phys. Lett.* **2005**, *409*, 295−299.
(27) Dyall, K. G. *Theor. Chem. Acc.* **2007**, *117*, 491−500.
(28) Rubinoff, D. S.; Evans, C. J.; Gerry, M. C. L. *J. Mol. Spectrosc.* **2003**, *218*, 169−179.
(29) Linstrom, P. J.; Mallard, W. G. *NIST Chemistry WebBook, NIST Standard Reference Database Number 69*; National Institute of Standards and Technology: Gaithersburg, MD, 2015.
(30) Simard, B.; James, A. M. *J. Chem. Phys.* **1992**, *97*, 4669−4678.
(31) Wang, F.; Le, A.; Steimle, T. C.; Heaven, M. C. *J. Chem. Phys.* **2011**, *134*, 031102.
(32) Le, A.; Heaven, M. C.; Steimle, T. C. *J. Chem. Phys.* **2014**, *140*, 024307.
(33) Teodoro, T. Q.; Haiduke, R. L. A.; Visscher, L. *Phys. Rev. A: At., Mol., Opt. Phys.* **2015**, *91*, 032516.

DOI: 10.1021/acs.jctc.6b00650
J. Chem. Theory Comput. 2017, 13, 1094−1101